International Journal of Supportive Research (IJSR), ISSN: 3079-4692
Volume 3, Issue 1, January-June, 2025, Available online at: www.ijsupport.com

Development of typical-element-doped functional π-systems consisting of naphthalene monoimide units

Dr. S.K. Mishra

Principal, S. Sinha College, Aurangabad

Keywords: Naphthalene monoimide, Typical element, Functionalized π-system, n-Type semiconductor

INTRODUCTION

π-Conjugated molecules are key components of advanced materials such as organic-based electronics. The function of these compounds is closely related tontheir delocalized π-electrons, which can be precisely modulated by introducing functional groups on the periphery of the compound. The characteristics of such designed molecules strongly rely on the inherent electronic nature of the parent skeleton, highlighting the importance of selecting an appropriate motif molecule. Such π-conjugated molecules should satisfy two criteria: (1) they intrinsically exhibit desirable electronic properties and (2) their structures are readily transformable via well-established organic transformations. π-Conjugated molecules are intrinsically electrondonors because the π-electrons are loosely bound to the core. Electron-accepting π-systems are thus relatively rare, underlining the need to develop novel electronaccepting π-systems. Furthermore, electron-accepting π-systems are attractive because high electron affinity leads to excellent atmospheric stability, electrontransporting properties, and short molecular contacts, all useful features for the construction of nextgeneration materials such as organic-based electronics and supramolecular assemblies.

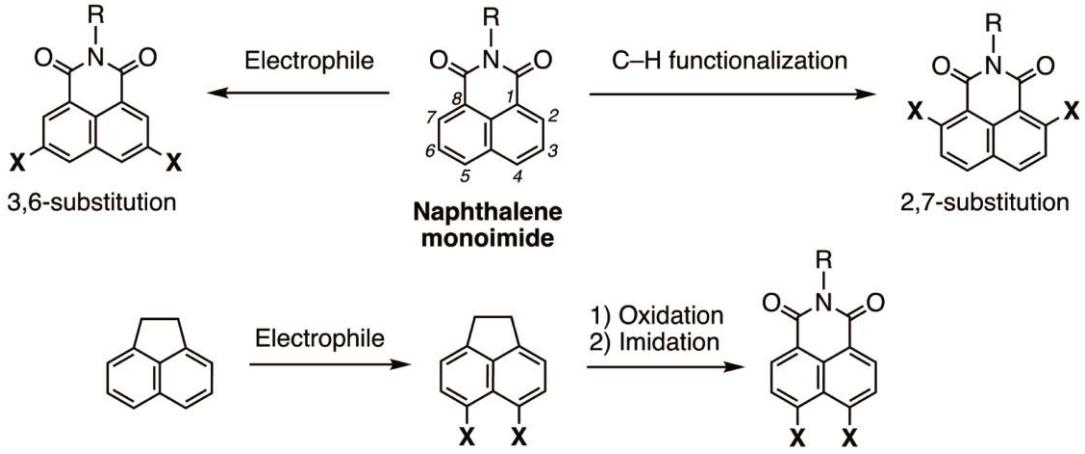

Figure 1. Syntheses of peripherally functionalized NMIs.

My research has focused on naphthalene monoimide (NMI) as a motif to create novel electron-accepting π-systems, due to its several advantageous features. First, various synthetic strategies to peripherally functionalized NMIs have been developed (**Figure 1**). The electrophilic aromatic substitution of NMI selectively affords the 3,6-functionalized derivative, with the transitionmetal- catalyzed direct C–H functionalization reaction proceeding at the *ortho*-positions of the carbonyl group (2,7-positions).[1] The 4,5-functionalized NMIs are accessible via two-step transformations from acenaphthene: electrophilic substitution followed by imidation. The second feature of NMI is the high electron affinity derived from the imide group, with π-extended analogues such as perylene bisimide (PBI) exhibiting excellent electron transporting properties in the solid state.[2] Donor-functionalized NMI derivatives exhibit solvatochromism in response to solvent polarity, which is useful for designing environment-responsive bioimaging luminophores.[3]

The third attractive feature of NMI is that its solid-state arrangement can be controlled precisely by changing the imide-substituents. This strategy has been frequently utilized in the development of high performance organic semiconductors and functional supramolecular assemblies.[4] Given the above, we selected NMI as the starting compound and applied our original molecular design guidelines for creating novel functional π-conjugated molecules. Herein, we introduce two strategies for generating useful high electron affinity compounds (**Figure 2**). In the first strategy, two NMI units are linked by a reactive moiety at the 4-positions, and then the linked complex is subjected to annulation at the 5-position to provide element-inserted PBIs as new nonplanar PBI derivatives. In the second strategy, we extended the π-system of NMI by introducing electronegative iminetype nitrogen atoms, allowing the dual incorporation of imide groups and imine-type nitrogen atoms to provide extremely high electron affinity.

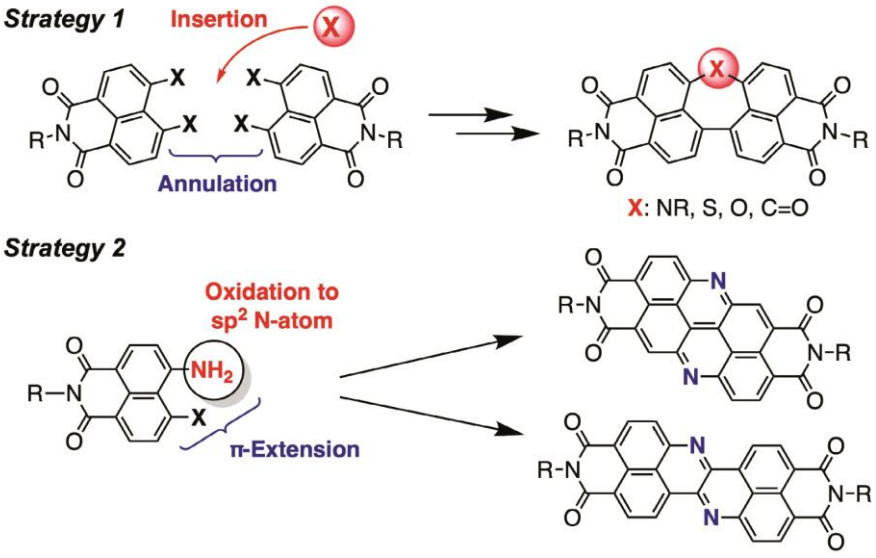

2. Element-inserted PBIs

PBI adopts a rigid, planar structure with attractive photophysical properties and high electron affinity, but the planar structure and high electron-deficiency enhance intermolecular interactions, resulting in low solubility in common organic solvents. In contrast, twisted PBI derivatives have a nonplanar structure due to steric repulsion at the bay area, and exhibit high solubility.[5–8] Such nonplanar PBIs function as solution-processable n-type organic semiconductors and non-fullerene electrontransporting materials for use in organic solar cells. We therefore proposed a new strategy for designing nonplanar PBI derivatives by inserting various elements at the linkage site. This section describes the synthesis and properties of nitrogen-, sulfur-, oxygen-, and carboninserted PBIs.

2-1. Insertion of nitrogen

The introduction of an electron-rich amine-type nitrogen atom on highly electron-accepting PBI cores confers intramolecular charge transfer (ICT) properties, providing molecules that undergo large conformational changes in the photoexcited state and a large dipole moment, two features important for stimuli-responsive molecules.[9] The NH group also acts as a hydrogenbonding donor. The substituent on the nitrogen atom controls the solid-state arrangement, essential for the design of effective electron transport materials for organic solar cells.[10,11] Then, we have designed a nitrogen-inserted PBI derivative.[12]

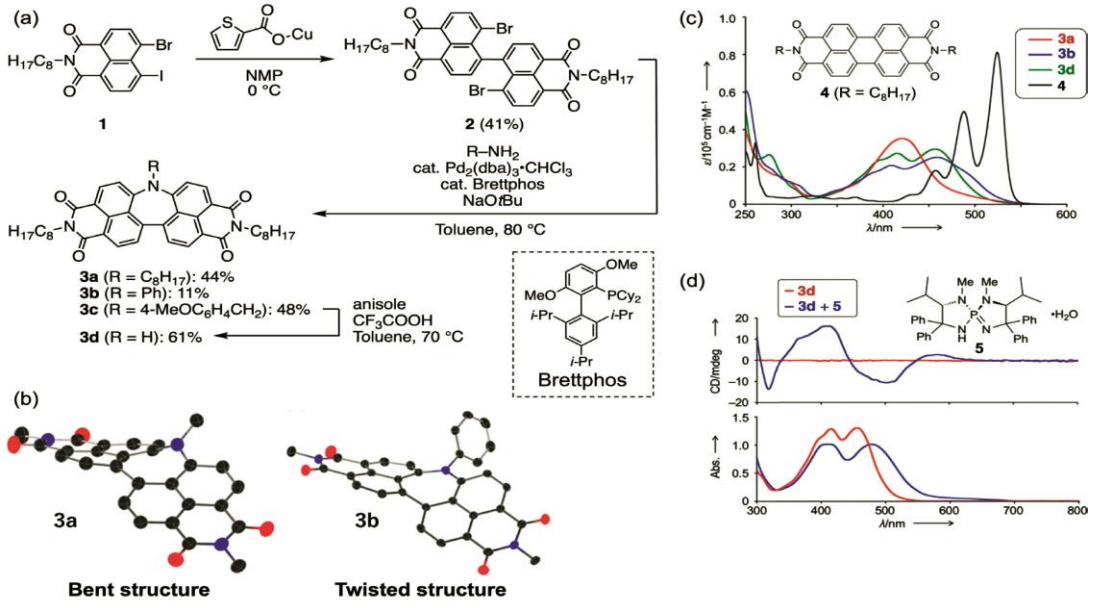

Figure 3. (a) Synthesis of nitrogen-inserted PBIs.
(b) X-ray crystal structure of 3a and 3b. Alkyl groups on the nitrogen atom are partially omitted.
(c) UV/vis absorption spectra of PBI and nitrogen-inserted PBIs.
(d) Chirality induction of NH-inserted 3d with optically active hydrogen-bonding acceptor 5.

Figure 3a shows the synthesis of nitrogen-inserted PBIs. An intermolecular C–I/C–I homo coupling reaction of 4-bromo-5-iodo-NMI **1** using copper(I) 2-thiophenecarboxylate provided the corresponding dimers **2**. Buchwald–Hartwig amination of **2** with octylamine, aniline, and 4-methoxybenzylamine afforded the corresponding nitrogen - inserted compounds **3a**, **3b**, and **3c**, respectively. Treatment of **3c** with an excess of anisole and trifluoroacetic acid deprotected the 4-methoxybenzyl group to provide NH inserted compound **3d** X-ray structural analysis revealed that octylamineinserted **3a** and aniline-inserted **3b** adopt different nonplanar structures (Figure 3b). Compound **3a** has a folded structure in which the two NMI units are not equivalent, whereas compound **3b** adoptsa symmetrically twisted structure. The structural difference between these two molecules was evident in their absorption spectra: octylamine-inserted **3a** exhibited a red-shifted absorption spectrum compared to aniline-inserted **3b** (Figure 3c). Interestingly, the structure of the nitrogen-inserted PBI can be controlled by external stimuli, such as by applying an electric field or adding hydrogen-bonding acceptors. Octylamine-inserted **3a** has a dipole moment because the two NMI moieties are not equivalent due to its folded structure. The application of an external electric field modulated the structural dynamics of **3a**. NH-inserted derivative **3d** functioned as a hydrogenbonding donor toward chiral iminophosphorane **5**,13 a compound developed by Prof. Ooi and Prof. Uraguchi. Treatment of **3d** with **5** provided a complex in toluene whose CD spectrum exhibited a Cotton effect (Figure 3d), indicating that complex formation with a chiral hydrogen-bonding acceptor controls the direction of helicity in NH-inserted PBI **3d**. During the above study, we also synthesized a nitrogen-bridged NMI dimer **8**, which exhibits aggregation-induced emission (AIE) (Figure 4).14 The key to generating AIE is the suppression of nonradiative deactivation via a twisted ICT (TICT) structure in the solid. Selective functionalization at the ortho-position of the carbonyl groups of 8 enabled tuning of the emission color to provide red-emission. Recently, Prof. Xia and co-workers revealed that photoexcitation of 8 induces symmetry-breaking charge transfer.1

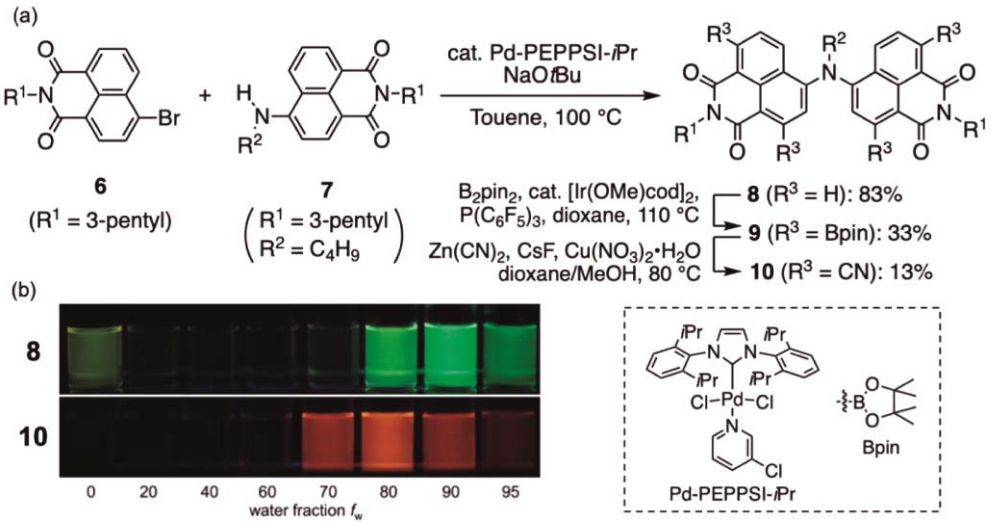

Figure 4. (a) Synthesis of nitrogen-bridged NM. (b) Photographs of THF/water solutions under photoirradiation

2-2. Insertion of sulphur

Several organosulfur compounds undergo sulfurextrusion reactions upon photoirradiation and/or heating. For example, thiepine undergoes a thermally induced pericyclic reaction to provide benzene following intermolecular collision.16,17 Photoirradiation of a 9-to-9' sulfoxide-bridged anthracene dimer gives 9,9'-bianthracene (Figure 5).18 We found that sulfurinserted PBIs undergo sulfur extrusion reactions to give PBIs.19 This unique reaction strategy enables fabrication of thin films of PBI by solution processing.

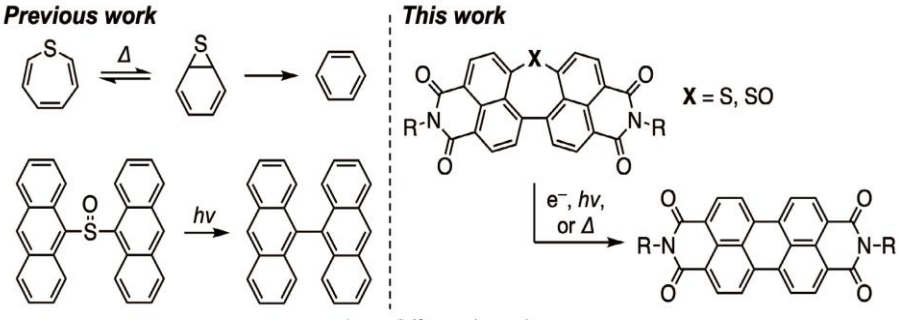

Figure 5. Sulfur extrusion reactions.

The synthetic strategies for sulfur-inserted PBI and the corresponding sulfoxide and sulfone are shown in Figure 6a. The nucleophilic aromatic substitution of 5,5'-bridged-4,4'-dibromo-NMI dimer **2** with sodium sulfide afforded sulfur-inserted PBI **11**. The sulfur unit of **11** was oxidized with *m*-chloroperoxybenzoic acid (*m*CPBA) to afford the corresponding sulfoxide **12**, whereas the tungsten-catalyzed oxidation20 of **11** with hydrogen peroxide provided sulfone **13**. We have also developed a gram-scale synthetic strategy to access sulfur-inserted PBIs for the efficient synthesis of analogues with different substituents at the imide positions for imidization in the final step. [21]

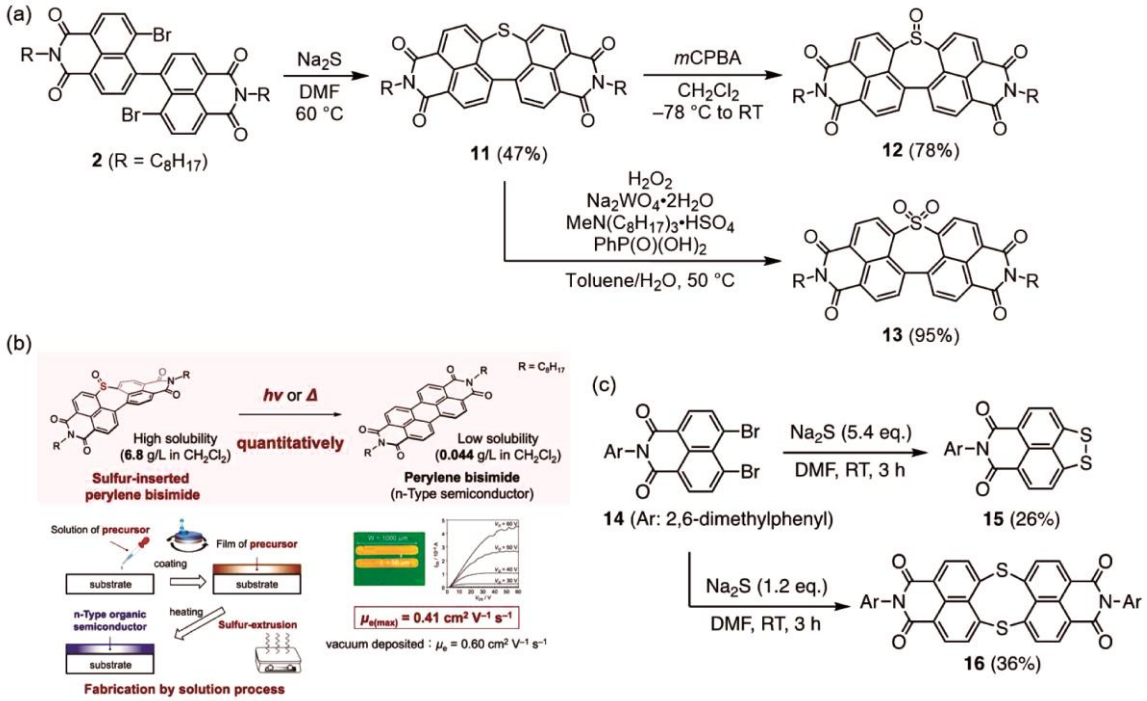

Figure 6. (a) Synthesis of sulfur-inserted PBIs.
(b) Fabrication of a thin film of PBI using sulfur-inserted PBI as a soluble precursor.
(c) Synthesis of doubly sulfur-inserted PBI.

Single-crystal X-ray analysis revealed that sulfur-inserted PBI adopts a nonplanar structure and accordingly sulfur-inserted PBI showed high solubility in common organic solvents. For example, the solubilities of sulfide-, sulfoxide-, and sulfone-inserted PBIs in dichloromethane are 2.9 g/L, 0.51 g/L, and 5.4 g/L, respectively, which are 150–1700 times higher than that of PBI (0.0033 g/L). Furthermore, subjecting sulfur-inserted PBI to photoirradiation, heating, and electron injection resulted in sulfur-extrusion reactions to afford PBI almost quantitatively. Finally, we examined the use of sulfur-inserted PBIs as a soluble precursor for PBI in collaboration with Prof. Yamada and Dr. Matsuo (Figure 6b). Sulfoxide-inserted PBI was spin-coated onto a silicon substrate, and the obtained thin film was heated to induce the sulfur-extrusion reaction. The devices acted as n-type semiconductors with a maximum electron mobility value of μe = 0.41 cm2 V–1 s–1, comparable to that obtained by vacuum deposition (μe = 0.6 cm2 V–1 s–1).

We also synthesized a doubly sulfur-inserted PBI derivative that adopts a V-shaped structure **(**Figure 6c).22 The activation energy for inversion of the V-shaped structure is 30 kcal mol–1. Disulfide-bridged NMI **15** was obtained as a by-product. Prof Xia and co-workers revealed that compound **15** undergoes ultrafast internal conversion by stretching the S–S bond.23

2-3. Insertion of oxygen

The synthetic procedure for oxygen-inserted PBI is shown in Figure 7. The reaction of 5,5'-bridged-4,4'-dichloronaphthalene dicarboxylic anhydride dimer **17** with 2,4,6 trimethylaniline afforded imide-substituted compound **18**. Subsequently, oxygen-inserted PBI was synthesized by reaction with α-benzaldoxyme24 under basic conditions.25 Interestingly, oxygen-inserted PBI **19** underwent an oxygen-extrusion reaction upon electron injection with decamethylcobaltocene affording the radical anion of PBI. The crude mixture was treated with *p*-chloranil, giving PBI **20** in 63% yield. The dissociation energy of a C–O bond is quite high, and the Lewis basicity of the oxygen atom in diaryl ethers is low. Consequently, cleavage of a C–O bond is challenging.[26,27] Our results provide fundamental insights into the development of a rational method for C–O bond transformation.

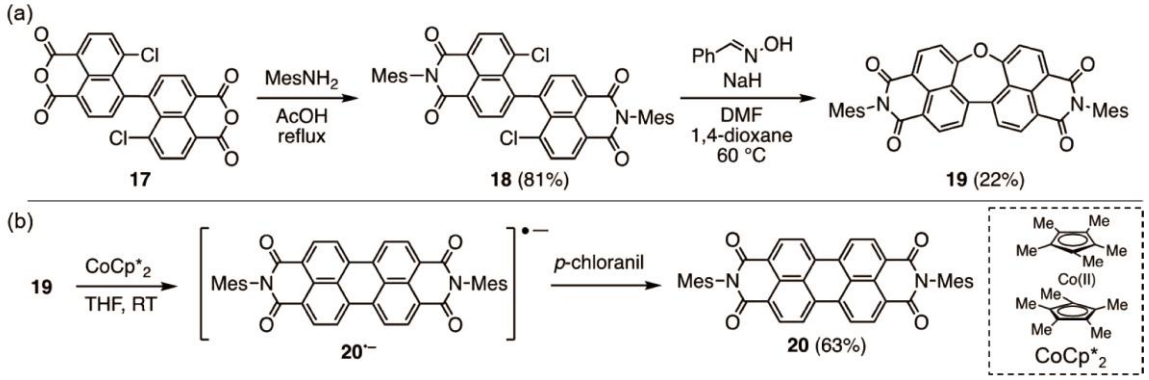

Figure 7. (a) Synthesis of oxygen-inserted PBI. (b) Oxygen-extrusion reaction via electron injection into oxygen-inserted PBI.

2-4. Insertion of carbon

Figure 8 shows the synthesis of carbon-inserted PBI. Treating 5,6-dibromoacenaphthene **21** with 1.0 equivalent of *n*-butyllithium afforded the corresponding mono-lithiated intermediate, which was coupled with 5-bromo-6-formylacenaphthene **22** to furnishbis(6-bromoacenaphthen-5-yl)methanol **23**. After oxidation of all the benzylic carbons in **23** with sodium dichromate, the reaction mixture was directly treated with 2,4,6-trimethylaniline to furnish the corresponding carbonyl-bridged NMI dimer. Intramolecular Yamamoto coupling of **24** with bis(1,5-cyclooctadiene)nickel(0) provided carbonyl-inserted PBI **25**.28 The carbonyl group was converted to a methylene group via Luche reduction, followed by treatment of triethylsilane and trifluoromethanesulfonic acid to provide methyleneinserted PBI **27**.

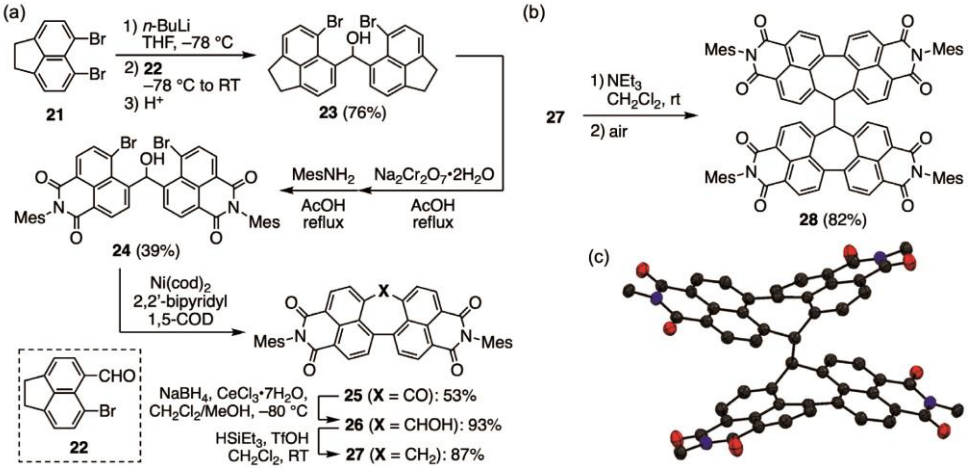

Figure 8. (a) Synthesis of carbon-inserted PBIs. (b) Reactivity of methylene-inserted PBI. (c) X-ray crystal structure of dimer 28.

X-ray structural analysis revealed that both carbonyl-andmethylene-inerted PBIs adopt nonplanar structures. Methylene-inserted PBI showed fluorescence with a quantum yield of 31%, whereas carbonyl-inserted PBI exhibited weak fluorescence with a quantum yield of 0.8%. Transient absorption spectroscopy suggested that photoirradiation of carbonyl-inserted **25** provided the excited triplet species. Interestingly, the deprotonation of methyleneinserted PBI **27** followed by aerobic oxidation furnished dimer **28**, whose central methylene carbons are connected. This dimer **28** exhibited reversible C–C bond formation under electrochemical redox conditions (a *dyrex* reaction).

3. DUAL INCORPORATION OF IMINE-TYPE NITROGEN ATOMS AND IMIDE SUBSTITUENTS

There are two general approaches for designing highly electron-accepting π-systems. One is the introduction of electron-withdrawing peripheral substituents such as an imide group, as seen in PBI, and the second is the introduction of electronegative sp^2-nitrogen atoms into the π-cores, as observed for an imine-doped pentacene that works as an n-type semiconductor.29 The two strategies have generally been applied independently, although there are several reports of the incorporation of both an electron-withdrawing group and an imine-type nitrogen atom.[30,31] The latter resulting

molecules show remarkably high electron affinity and work as an effective and airstable n-type organic semiconductor. These findings prompted us to incorporate both an electron withdrawing group and an imine-type nitrogen atom into anthanthrene and zethrene.

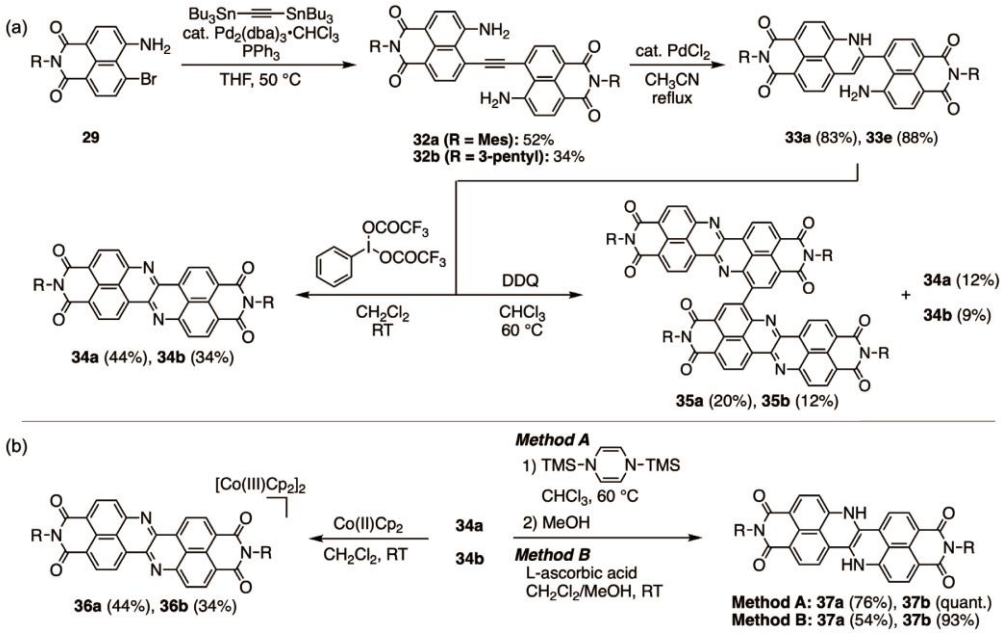

Figure 9. Guidelines for designing electron-accepting π-systems. (a) Incorporation of imide substituents and imine-type nitrogen atoms.
(b) Previously reported molecules incorporating both an imide substituent and imine-type nitrogen atoms.

3-1. Acridino[2,1,9,8-*klmna*]acridine bisimide

Anthanthrene is a nanographene with a zig-zag edge structure32 and exhibits excellent photophysical properties and charge-transport behavior derived from its large π-system, leading to anthanthrene derivatives being studied as hole-transporting materials in organic solar cells.33 Anthanthrene is thus potentially attractive as a building block for organic electronic materials. We previously designed acridino[2,1,9,8-*klmna*]acridine bisimide (AABI), which represents an anthanthrene derivative that incorporates both imide groups and imine-type nitrogen atoms.34 The synthesis of AABI is shown in Figure 10. Nickel-catalyzed homo-coupling of 4-bromo-5- amino NMI **29** provided the corresponding dimer
30. Subsequent oxidation with 2,3-dichloro-5,6- dicyanobenzoquinone and Sc(OTf)3 afforded AABI **31**. Electrochemical analysis showed that AABI exhibits a first reduction potential at –0.72 V (vs. Fc/Fc+). In the solid state, *N*-alkyl derivatives adopt brickworktype packing. Organic field-effect transistor (OFET) devices comprising AABI were fabricated by vacuum deposition. Phenethyl derivatives **31c** afforded a maximum electron mobility μmax of 0.34 cm2 V –1 s–1, and single-crystal OFET devices showed a high electron mobility μe of 0.90 cm2 V –1 s–1. Thus, the incorporation of imide groups and imine-type nitrogen atoms is conducive to the formation of robust n-type semiconductor molecules.

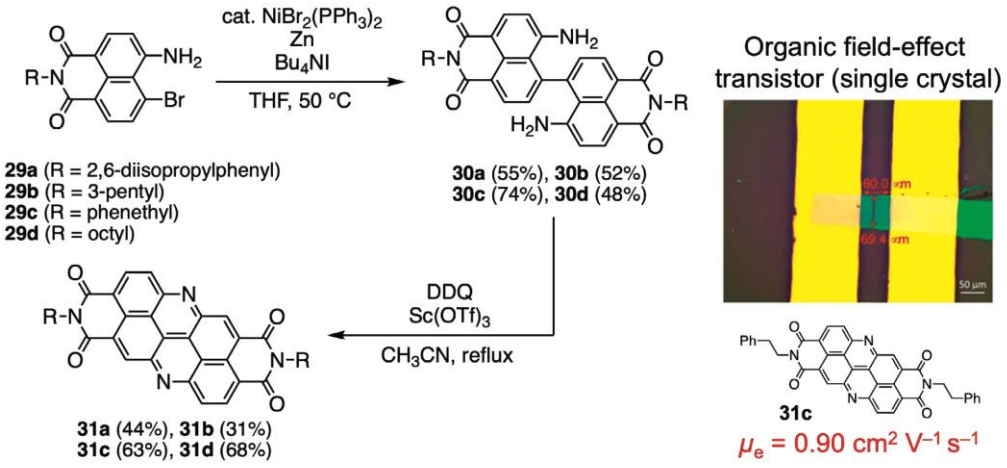

Figure 10. Synthesis and single-crystal OFET device comprising AABI.

3-2. Diazazethrene bisimide

Zethrene is a nanographene with a high reduction potential of –1.76 V,35 which is more positive than that of anthanthrene (–2.11 V).32 We formed an extremely electron-accepting π-system by functionalizing zethrene with imide groups and imine-type nitrogen atoms. [36]

The synthetic procedure is shown in Figure 11. Migita–Kosugi–Stille cross-coupling of 4-amino-5- bromo NMI **29** with bis(trimethylstannyl)acetylene afforded alkyne-bridged dimer **32**. Pd-catalyzed intramolecular hydroamination of **32** gave enamineform **33**. Treatment of **33** with bis(trifluoroacetoxy)- iodobenzene provided diazazethrene bisimide **34**. Interestingly, subjecting compound **33** to oxidation with DDQ provided not only compound **34** but also dimer **35**. Electrochemical measurements showed that diazazethrene bisimide and its dimer exhibit first reduction potentials at –0.49 V and –0.36 V, respectively. Electron injection into diazazethrene bisimide **34** using cobaltocene afforded the dianion **36**, which is remarkably stable under ambient conditions. Treatntofdiazazethrene bisimide **34** with bis(trimethylsilyl)dihydropyrazine afforded dihydroform **37**. Interestingly, this hydrogenation could be induced using L-ascorbic acid, a weak reductant. Dihydro-form **37** and dianion **36** were reversibly transformed by the addition of acid and base. A vacuum-deposited field-effect transistor comprising 34b was fabricated and exhibited a maximum electron mobility μe of 6.7 × 10–3 cm2 V –1 s–1 in vacuum and μe = 5.4 × 10–3 cm^2 V –1 s–1 in air. The observed excellent mobility under air is likely due to the high electron affinity of diazazethrene bisimide.

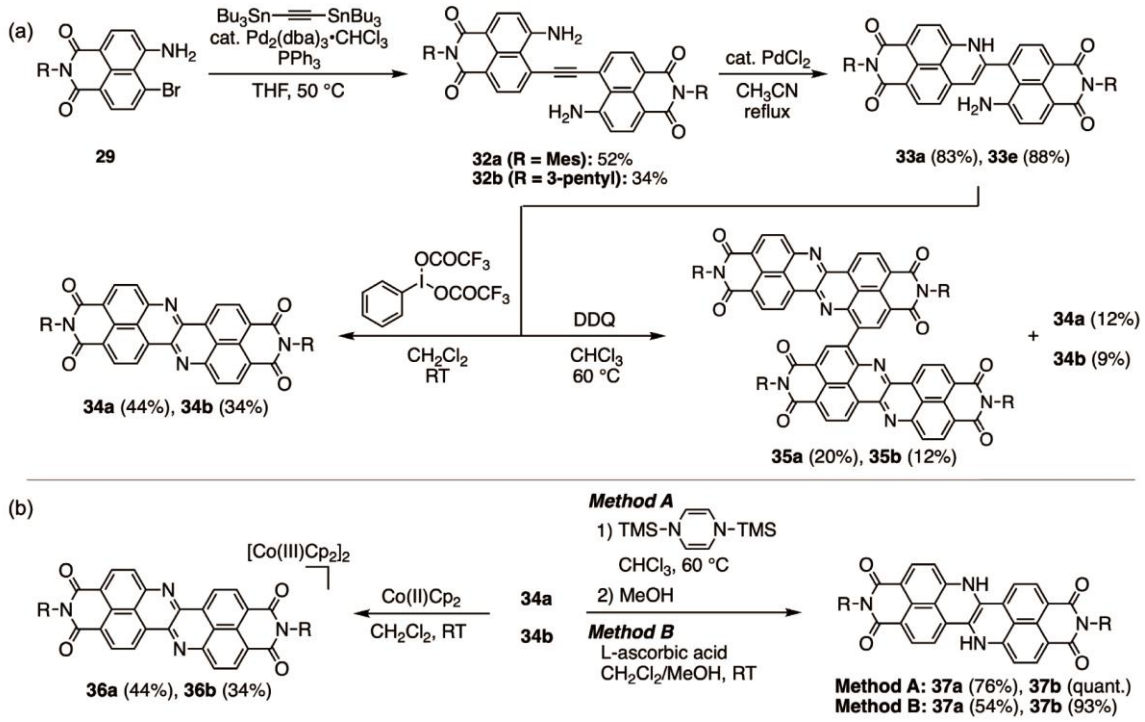

Figure 11. (a) Synthesis of diazazethrene bisimides and their dimers. (b) Reduction of diazazethrene bisimides.

SUMMARY

This account summarized our developmental studies of novel functionalized π-systems using NMI as a building block. Section 2 presented elementinserted PBI derivatives with nitrogen, sulfur, carbon, and oxygen atoms. These compounds exhibit unique functions due to cooperation between the inserted elements and the compound's nonplanarity. Sulfurinserted PBI functioned as a soluble precursor for PBI, enabling the fabrication of an n-type semiconductor film using a solution process. In Section 3, we described the incorporation of imide- and imine-type nitrogen atoms into two nanographenes: anthanthrene and zethrene. The resulting compounds exhibit excellent electron affinity and thus function as effective n-type semiconductor materials.

ACKNOWLEDGMENTS

I would like to extend my heartiest thanks to Prof. U.S. Yadav Retd. HOD, Deptt. of Chemistry, J.P.U. Chapra, Prof. Rabindra Singh, Deptt. of Chemistry, J.P.U. Chapra, Prof. Brij Bihari Sharma, Retd. HOD, Deptt. of Chemistry, M.U. Bodhgaya, Prof. R.P.S. Chauhan, Retd. HOD, Deptt. of Chemistry, M.U. Bodhgaya, Prof. Udai Arbind, Deptt. of Chemistry, J.P.U. Chapra, for providing academic support and valuable suggestions for doing so and impetus force for moving ahead.

REFERENCES

[1] A. I. Wright, B. M. Kariuki, Y.-L. Wu, *Eur. J. Org. Chem*. **2021**, *2021*, 4647.
[2] Z. Liu, G. Zhang, Z. Cai, X. Chen, H. Luo, Y. Li, J. Wang, D. Zhang, *Adv. Mater*. **2014**, *26*, 6965.
[3] H.-Q. Dong, T.-B. Wei, X.-Q. Ma, Q.-Y. Yang, Y.-F. Zhang, Y.-J. Sun, B.-B. Shi, H. Yao, Y.-M. Zhang, Q. Lin, *J. Mater. Chem. C* **2020**, *8*, 13501.
[4] Q. Lin, X.-W. Guan, S.-S. Song, H. Fan, H. Yao, Y.-M. Zhang, T.-B. Wei, *Polym. Chem*. **2019**, *10*, 253.
[5] F. Würthner, *Pure Appl. Chem*. **2006**, *78*, 2341.
[6] H. Qian, Z. Wang, W. Yue, D. Zhu, *J. Am. Chem. Soc*. **2007**, *129*, 10664.
[7] H. Qian, F. Negri, C. Wang, Z. Wang, *J. Am. Chem. Soc*. **2008**, *130*, 17970.
[8] W. Jiang, L. Ye, X. Li, C. Xiao, F. Tan, W. Zhao, J. Hou, Z. Wang, *Chem. Commun*. **2014**, *50*, 1024.
[9] M. Hirai, N. Tanaka, M. Sakai, S. Yamaguchi, *Chem. Rev*. **2019**, *119*, 8291.
[10] H. Langhals, S. Kirner, *Eur. J. Org. Chem*. **2000**, *2000*, 365.
[11] A. D. Hendsbee, J.-P. Sun, W. K. Law, H. Yan, I. G. Hill, D. M. Spasyuk, G. C. Welch, *Chem. Mater*. **2016**, *28*, 7098.
[12] S. Hayakawa, A. Kawasaki, Y. Hong, D. Uraguchi, T. Ooi, D. Kim, T. Akutagawa, N. Fukui, H. Shinokubo, *J. Am. Chem. Soc*. **2019**, *141*, 19807.
[13] D. Uraguchi, Y. Ueki, T. Ooi, *Science* **2009**, *326*, 120.
[14] K. Tajima, N. Fukui, H. Shinokubo, *Org. Lett*. **2019**, *21*, 9516.
[15] X. Niu, K. Tajima, J. Kong, M. Tao, N. Fukui, Z. Kuang, H. Shinokubo, A. Xia, *Phys. Chem. Chem. Phys*. **2022**, *24*, 14007.
[16] J. M. Hoffman Jr., R. H. Schlessinger, *J. Am. Chem. Soc*. **1970**, *92*, 5263.
[17] R. Gleiter, G. Krennrich, D. Cremer, K. Yamamoto, I. Murata, *J. Am. Chem. Soc*. **1985**, *107*, 6874.
[18] P. R. Christensen, B. O. Patrick, E. Caron, M. O. Wolf, *Angew. Chem., Int. Ed*. **2013**, *52*, 12946.
[19] S. Hayakawa, K. Matsuo, H. Yamada, N. Fukui, H. Shinokubo, *J. Am. Chem. Soc*. **2020**, *142*, 11663.
[20] K. Sato, M. Hyodo, M. Aoki, X.-Q. Zheng, R. Noyori, *Tetrahedron* **2001**, *57*, 2469.
[21] Y. Tanaka, K. Matsuo, H. Yamada, N. Fukui, H. Shinokubo, *Eur. J. Org. Chem*. **2022**, e202200770.
[22] Y. Tanaka, K. Tajima, N. Fukui, H. Shinokubo, *Asian J. Org. Chem*. **2021**, *10*, 541.
[23] Z. Wang, R. Jing, Y. Li, D. Song, Y. Wan, N. Fukui, H. Shinokubo, Z. Kuang, A. Xia, *J. Phys. Chem. Lett*. **2023**, *14*, 8485.
[24] A. Nishiyama, M. Fukuda, S. Mori, K. Furukawa, H. Fliegl, H. Furuta, S. Shimizu, *Angew. Chem., Int. Ed*. **2018**, *57*, 9728.
[25] M. Odajima, N. Fukui, H. Shinokubo, *Org. Lett*. **2023**, *25*, 282.
[26] H. Xu, B. Yu, H. Zhang, Y. Zhao, Z. Yang, J. Xu, B. Han, Z. Liu, *Chem. Commun*. **2015**, *51*, 12212.
[27] N. Haga, H. Takayanagi, *J. Org. Chem*. **1996**, *61*, 735.
[28] T. Yamamoto, S. Wakabayashi, K. Osakada, *J. Organomet. Chem*. **1992**, *428*, 223.
[29] Q. Miao, *Synlett* **2012**, *23*, 326.
[30] H. Li, F. S. Kim, G. Ren, E. C. Hollenbeck, S. Subramaniyan, S. A. Jenekhe, *Angew. Chem. Int. Ed*. **2013**, *52*, 5513.
[31] T. Okamoto, S. Kumagai, E. Fukuzaki, H. Ishii, G. Watanabe, N. Niitsu, T. Annaka, M. Yamagishi, Y. Tani, H. Sugiura, T. Watanabe, S. Watanabe, J. Takeya, *Sci. Adv*. **2020**, *6*, eaaz0632.
[32] Y. Gu, X. Wu, T. Y. Gopalakrishna, H. Phan, J. Wu, *Angew. Chem. Int. Ed*. **2018**, *57*, 6541.
[33] L. Zhang, B. Walker, F. Liu, N. S. Colella, S. C. B. Mannsfeld, J. J. Watkins, T.-Q. Nguyen, A. L. Briseno, *J. Mater. Chem*. **2012**, *22*, 4266.
[34] K. Tajima, K. Matsuo, H. Yamada, S. Seki, N. Fukui, H. Shinokubo, *Angew. Chem. Int. Ed*. **2021**, *60*, 14060.
[35] L. Shan, Z. Liang, X. Xu, Q. Tang, Q. Miao, *Chem. Sci*. **2013**, *4*, 3294.
[36] K. Tajima, K. Matsuo, H. Yamada, N. Fukui, H. Shinokubo, *Chem. Sci*. **2023**, *14*, 635.